

Reactive Power Availability of a 20 kW Three Phase Three Level PFC

Akshay Mahajan, Christoph Siedle
FRAUNHOFER INSTITUTE FOR SOLAR ENERGY SYSTEMS ISE
Heidenhofstrasse 2
Freiburg im Breisgau, Germany
Phone: +49 (761) 4588-5088
Fax: +49 (761) 4588-0
Email: akshay.mahajan@ise.fraunhofer.de
URL: <http://www.ise.fraunhofer.de>

Keywords

«Power factor correction», «Modelling», «Converter control», «Charging Infrastructure for EVs», «Multilevel converters»

Abstract

Three phase rectifiers are gaining importance with the increase in charging infrastructure demand for EVs. This paper proves the reactive power availability of a three phase three level unidirectional rectifier consisting only two active switches per phase, with a power factor up to ± 0.9 . Each phase leg of the converter is connected to the grid with a L-C-L filter and the filter star point of the capacitors is connected to the middle point of the DC link. The neutral of the grid being not connected to the start point of the filter capacitors enables start point modulation. In this paper, a current controller is proposed for the star point modulation with two main objectives; achieving a desired power factor and minimizing the DC link voltage. Detailed mathematical derivations and simulation results proving the reactive power availability of the converter are presented.

Introduction

When it comes to reactive power, grid connected converters have to comply with certain standards. The standard [1] states that a grid connected converter with power rating ≥ 4.6 kVA should be able to exchange reactive power with a power factor up to 0.9. This is possible for topologies operating in bidirectional single or three phase power converters. On the other hand, the improved performance of three level converters compared to two level converters is discussed in detail in [2]. Three phase three level bidirectional converters have typically four or more switches per phase [2]. This increases the costs for switches, gate drivers and associated peripheries. Reactive power availability of a topology (delta-switch rectifier) with only two active switches per phase is shown in [3]. But this topology has two level characteristics and the switches are subjected to full DC link voltage.

This paper proves the reactive power availability of a three phase three level unidirectional rectifier. This restricts its operation in one direction but is suitable for unidirectional charging applications. Further, unidirectional chargers with reactive power availability have been investigated for reactive power support to the grid in [4] showing higher EV penetration and their contribution to grid stability.

Operation principle

The topology of the three phase three level power factor correction converter (hereafter referred as 3L-PFC) is shown in Fig.1. It consists of two IGBTs and four diodes per phase. With only two IGBTs per phase, only six gate drivers are required. The twelve diodes altogether enable only unidirectional

operation of this converter. The active power can only be transferred from the grid to the DC link. The DC link is the addition of two voltage sources in series as shown in Fig.1. The three phases are connected to the grid through individual L-C-L filter. The star-point of the filter capacitors is connected to the middle point N of the DC link but is not connected to the neutral of the grid. Thus the filter star-point voltage can be modulated, which is essential for providing reactive power with this topology. The 3L-PFC is controlled through a state space controller providing a constant current to the DC link. The detailed operation of the state space controller is not in the scope of this paper. The maximum apparent power of the converter is 22 kVA.

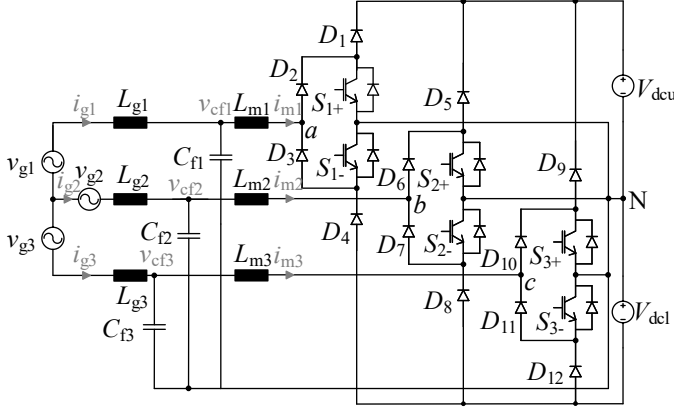


Fig. 1: 3L-PFC Topology

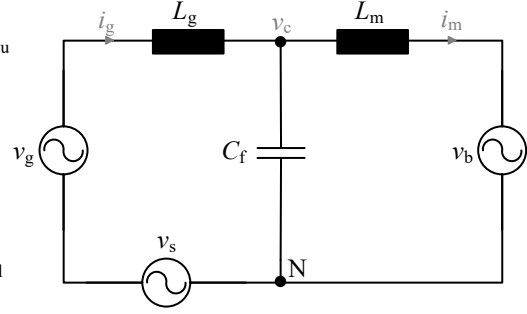


Fig. 2: Simplified representation of the 3L-PFC

A simplified representation of one leg of the 3L-PFC is shown in Fig. 2. Here v_g is the grid voltage, v_b is the bridge voltage, v_c is the filter capacitor voltage and v_s is the filter star-point voltage. To exchange reactive power with the grid, it is necessary to have a phase shift between v_g and i_g . On account of the diodes D_1 through D_{12} is not possible to create a phase shift between v_b and i_m . The product of $v_b(t)$ and $i_m(t)$ can only be positive. The idea proposed here is to shift the star-point N with respect to the grid neutral. This is achieved by controlling the voltage v_s for a desired power factor based on the grid current, bridge voltage and grid voltage through star point modulation. The voltage v_s consists of only triple fundamental frequency components.

Preliminary considerations

The star point modulation is based on the star point of the filter capacitors from the L-C-L filter and not on the neutral of the grid. For the sake of simplicity, it is assumed that the filter capacitors are connected in star configuration, where the star point is physically present. However, the equations governing star configuration can also be converted to the delta configuration, wherein the filter star point is only virtually available. The filter capacitor voltages being:

$$\underline{v_{cf}}(t) = \hat{V}_{cf} \cdot \begin{bmatrix} \sin(\omega \cdot t) \\ \sin(\omega \cdot t - \frac{2}{3} \cdot \pi) \\ \sin(\omega \cdot t + \frac{2}{3} \cdot \pi) \end{bmatrix} \quad \text{here} \quad \omega = (2 \cdot \pi \cdot 50) \text{ rad/s} \quad (1)$$

The reference value of the current through inductors L_{m1} , L_{m2} and L_{m3} are given below.

$$\underline{i_{m,ref}}(t) = \hat{I}_{m,ref} \cdot \begin{bmatrix} \sin(\omega \cdot t + \phi) \\ \sin(\omega \cdot t - \frac{2}{3} \cdot \pi + \phi) \\ \sin(\omega \cdot t + \frac{2}{3} \cdot \pi + \phi) \end{bmatrix} \quad \text{here} \quad -\frac{\pi}{6} \leq \phi \leq \frac{\pi}{6} \quad (2)$$

The required star point voltage in this case is:

$$v_s(t) = \sum_{n=1}^3 \left[(\text{sign}(v_{cf}(t)_n) \neq \text{sign}(i_{m,\text{ref}}(t)_n)) \cdot v_{cf}(t)_n \right] \quad (3)$$

A modulation with this star point voltage $v_s(\omega \cdot t)$ as shown in Fig. 3 cannot be realized since the voltage drop across the filter capacitor is a result of a current build up by the integration through the inductor L_m . Therefore, the voltage cannot change in triangular pulse pattern as seen in Fig. 3. However, application of such modulation voltage is possible in delta-switch rectifier [3]. In this work, the neutral point of the filter capacitors from the L-C-L shown in Fig. 4 has to be modulated with a sinusoidal voltage to achieve the reactive power transfer. A pulse-free voltage $v_{s,\text{sin}}(\omega \cdot t)$ shown in Fig. 5 is used for the star point

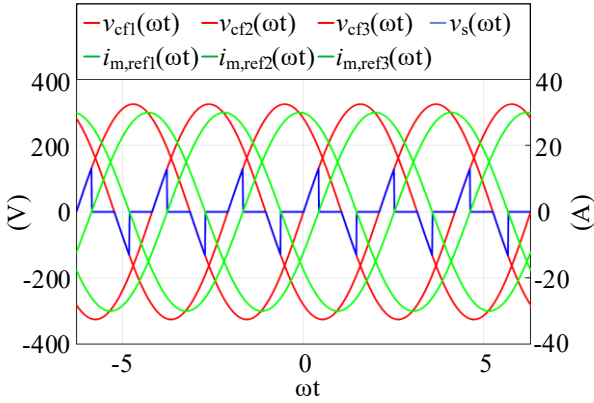


Fig. 3: Required v_s for phase shift between v_{cf} and $i_{m,\text{ref}}$

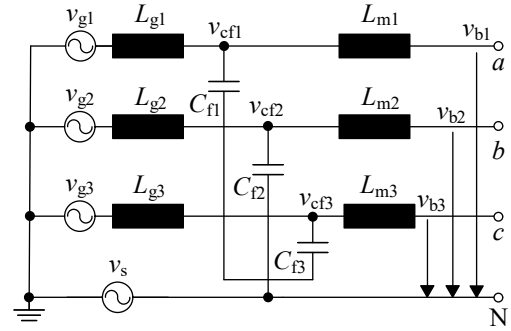


Fig. 4: L-C-L filter of the 3L-PFC

modulation since the voltage $v_s(\omega \cdot t)$ required for star point modulation can be exceeded.

$$v_{s,\text{sin}}(t) = -\hat{V}_{cf} \cdot \sin(\phi) \cdot \cos(3\omega \cdot t + 3\phi) \quad (4)$$

The bridge voltage $v_b(\omega \cdot t)$ with its limits fixed to the half of the DC link voltage results in current through the inductor L_m with a voltage drop equal to the difference between the filter capacitor voltage and the star point voltage. Lastly, because of the unidirectional power transfer, the instantaneous power must always be positive as shown in Fig. 6.

$$\underline{v}_b(t) = \underline{v}_{cf}(t) - \begin{bmatrix} 1 \\ 1 \\ 1 \end{bmatrix} \cdot v_{s,\text{sin}}(t) \quad (5)$$

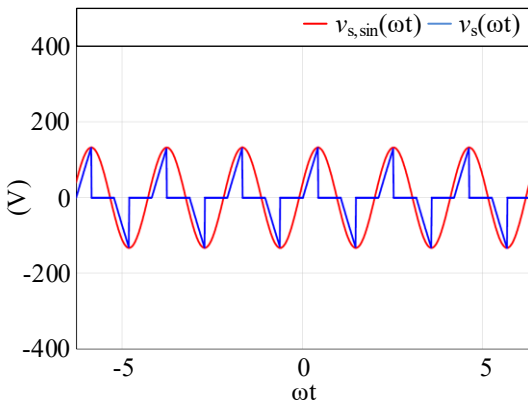


Fig. 5: Pulse-free sinusoidal star point voltage

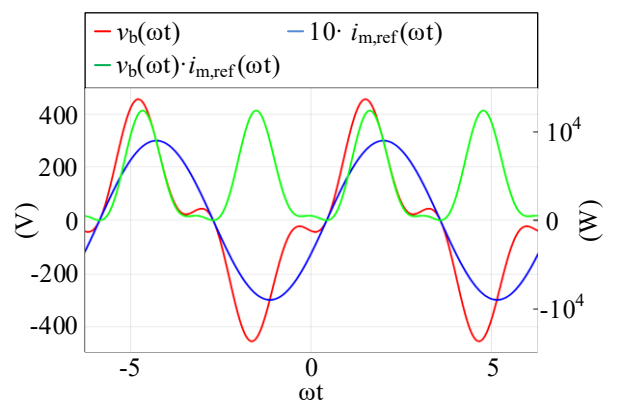


Fig. 6: Bridge parameters of one phase leg

Mathematical derivation

In this section, the mathematical equations are derived. It is necessary to derive mathematical relation between the different parameters in Fig. 2 with respect to the grid voltage. The modulation voltage v_s , maximum bridge voltage v_b and their respective phase angles are determined for a reference grid current and power factor.

$$\begin{aligned} v_g(t) &= \hat{V}_g \cdot \cos(\omega \cdot t) \\ i_g(t) &= \hat{I}_g \cdot \cos(\omega \cdot t + \phi) \\ v_s(t) &= \hat{V}_s \cdot \cos(3\omega \cdot t + \theta) \end{aligned} \quad (6)$$

The system is time invariant and the parameters having the components ω and 3ω can be calculated separately. The grid voltage and grid current should ideally have only components oscillating at the fundamental frequency. For identification, the parameters (bridge current i_m , bridge voltage v_b and the filter capacitor voltage v_{cf}) consisting of both the fundamental and triple fundamental frequency components are denoted with subscript '1' and '3' for the fundamental frequency and triple fundamental frequency components respectively. These indices are not the same as phases. Three variables namely the instantaneous value, peak value and the corresponding phase angle are to be determined for each of the parameters stated below. All phase angles in equation 7 are with respect to the grid voltage.

$$\begin{aligned} i_{m1}(t) &= \hat{I}_{m1} \cdot \cos(\omega \cdot t + \alpha_1) & i_{m3}(t) &= \hat{I}_{m3} \cdot \cos(3\omega \cdot t + \alpha_3) \\ v_{c1}(t) &= \hat{V}_{c1} \cdot \cos(\omega \cdot t + \beta_1) & v_{cf3}(t) &= \hat{V}_{cf3} \cdot \cos(3\omega \cdot t + \beta_3) \\ v_{b1}(t) &= \hat{V}_{b1} \cdot \cos(\omega \cdot t + \gamma_1) & v_{b3}(t) &= \hat{V}_{b3} \cdot \cos(3\omega \cdot t + \gamma_3) \end{aligned} \quad (7)$$

Firstly, the parameters with fundamental frequency components are evaluated. The following matrix in s domain is derived from the Fig. 2.

$$\begin{bmatrix} V_g(s) \\ V_{b1}(s) \end{bmatrix} = \begin{bmatrix} s \cdot L_g + \frac{1}{s \cdot C_f} & -\frac{1}{s \cdot C_f} \\ \frac{1}{s \cdot C_f} & -(s \cdot L_m + \frac{1}{s \cdot C_f}) \end{bmatrix} \begin{bmatrix} I_g(s) \\ I_{m1}(s) \end{bmatrix} \quad (8)$$

Transforming the matrix to derive bridge voltage and inductor current as a function of grid voltage and current current.

$$\begin{bmatrix} V_{b1}(s) \\ I_{m1}(s) \end{bmatrix} = \begin{bmatrix} s^2 \cdot C_f \cdot L_m + 1 & -s \cdot (s^2 \cdot C_f \cdot L_m \cdot L_g + (L_m + L_g)) \\ -s \cdot C_f & s^2 \cdot C_f \cdot L_g + 1 \end{bmatrix} \begin{bmatrix} V_g(s) \\ I_g(s) \end{bmatrix} \quad (9)$$

Replacing s with $j\omega$ and representing the parameters in complex domain.

$$\begin{bmatrix} \hat{V}_{b1} \cdot e^{j\gamma_1} \\ \hat{I}_{m1} \cdot e^{j\alpha_1} \end{bmatrix} = \begin{bmatrix} 1 - \omega^2 \cdot C_f \cdot L_m & -j \cdot \omega \cdot (L_m + L_g - \omega^2 \cdot C_f \cdot L_m \cdot L_g) \\ -j \cdot \omega \cdot C_f & 1 - \omega^2 \cdot C_f \cdot L_g \end{bmatrix} \begin{bmatrix} \hat{V}_g \\ \hat{I}_g \cdot e^{j\phi} \end{bmatrix} \quad (10)$$

$$\hat{V}_{b1} \cdot \cos(\omega \cdot t + \gamma_1) = (1 - \omega^2 \cdot C_f \cdot L_m) \cdot \hat{V}_g \cdot \cos(\omega \cdot t) + \omega \cdot (L_m + L_g - \omega^2 \cdot C_f \cdot L_m \cdot L_g) \cdot \hat{I}_g \cdot \sin(\omega \cdot t + \phi) \quad (11)$$

$$\hat{I}_{m1} \cdot \cos(\omega \cdot t + \alpha_1) = \omega \cdot C_f \cdot \hat{V}_g \cdot \sin(\omega \cdot t) + (1 - \omega^2 \cdot C_f \cdot L_g) \cdot (\hat{I}_g \cdot \cos(\omega \cdot t + \phi)) \quad (12)$$

Expanding the cosine and sine terms from equations 11 and 12.

$$\begin{pmatrix} \hat{V}_{b1} \cdot \cos(\gamma_1) \cdot \cos(\omega \cdot t) \\ \pm \hat{V}_{b1} \cdot \sin(\gamma_1) \cdot \sin(\omega \cdot t) \end{pmatrix} = \begin{pmatrix} (1 - \omega^2 \cdot C_f \cdot L_m) \cdot \hat{V}_g \cdot \cos(\omega \cdot t) + \\ \omega \cdot (L_m + L_g - \omega^2 \cdot C_f \cdot L_m \cdot L_g) \cdot \hat{I}_g \cdot \sin(\phi) \cdot \cos(\omega \cdot t) \\ + \omega \cdot (L_m + L_g - \omega^2 \cdot C_f \cdot L_m \cdot L_g) \cdot \hat{I}_g \cdot \cos(\phi) \cdot \sin(\omega \cdot t) \end{pmatrix} \quad (13)$$

$$\begin{pmatrix} \hat{I}_{m1} \cdot \cos(\alpha_1) \cdot \cos(\omega \cdot t) \\ + \hat{I}_{m1} \cdot \sin(\alpha_1) \cdot \sin(\omega \cdot t) \end{pmatrix} = \begin{pmatrix} (1 - \omega^2 \cdot C_f \cdot L_g) \cdot \hat{I}_g \cdot \cos(\phi) \cdot \cos(\omega \cdot t) + \\ \omega \cdot C_f \cdot \hat{V}_g \cdot \sin(\omega \cdot t) \\ -(1 - \omega^2 \cdot C_f \cdot L_g) \cdot \hat{I}_g \cdot \sin(\phi) \cdot \sin(\omega \cdot t) \end{pmatrix} \quad (14)$$

Comparing the coefficients of $\cos(\omega \cdot t)$ and $\sin(\omega \cdot t)$, equation 15 and 16 are derived.

$$\hat{V}_{b1} \cdot \cos(\gamma_1) = (1 - \omega^2 \cdot C_f \cdot L_m) \cdot \hat{V}_g + \omega \cdot (L_m + L_g - \omega^2 \cdot C_f \cdot L_m \cdot L_g) \cdot \hat{I}_g \cdot \sin(\phi) \quad (15)$$

$$\hat{V}_{b1} \cdot \sin(\gamma_1) = -\omega \cdot (L_m + L_g - \omega^2 \cdot C_f \cdot L_m \cdot L_g) \cdot \hat{I}_g \cdot \cos(\phi) \quad (16)$$

$$\hat{I}_{m1} \cdot \cos(\alpha_1) = (1 - \omega^2 \cdot C_f \cdot L_g) \cdot \hat{I}_g \cdot \cos(\phi) \quad (17)$$

$$\hat{I}_{m1} \cdot \sin(\alpha_1) = -\omega \cdot C_f \cdot \hat{V}_g + (1 - \omega^2 \cdot C_f \cdot L_g) \cdot \hat{I}_g \cdot \sin(\phi) \quad (18)$$

Dividing equation 15 by equation 16, angle γ_1 is obtained.

$$\gamma_1 = \operatorname{arccot} \left[-\frac{1 - \omega^2 \cdot C_f \cdot L_m}{\omega \cdot (L_m + L_g - \omega^2 \cdot C_f \cdot L_m \cdot L_g)} \frac{\hat{V}_g}{\hat{I}_g} \cdot \cos(\phi) - \tan(\phi) \right] \quad (19)$$

Substituting γ_1 in equation 16,

$$\hat{V}_{b1} = \left(\frac{\omega \cdot (L_m + L_g - \omega^2 \cdot C_f \cdot L_m \cdot L_g) \dots}{\sqrt{(\hat{I}_g \cdot \cos(\phi))^2 + \left[\hat{I}_g \cdot \sin(\phi) + \frac{1 - \omega^2 \cdot C_f \cdot L_m}{\omega \cdot (L_m + L_g - \omega^2 \cdot C_f \cdot L_m \cdot L_g)} \cdot \hat{V}_g \right]^2}} \right) \quad (20)$$

Substituting γ_1 and \hat{V}_{b1} in equation 7,

$$v_{b1}(t) = (1 - \omega^2 \cdot C_f \cdot L_m) \cdot \hat{V}_g \cdot \cos(\omega \cdot t) + \omega \cdot (L_m + L_g - \omega^2 \cdot C_f \cdot L_m \cdot L_g) \cdot \hat{I}_g \cdot \sin(\omega \cdot t + \phi) \quad (21)$$

Dividing equation 18 by 17, the angle α_1 is obtained.

$$\alpha_1 = \arctan \left[\tan(\phi) - \frac{\omega \cdot C_f \cdot \hat{V}_g}{(1 - \omega^2 \cdot C_f \cdot L_g) \cdot \hat{I}_g \cdot \cos(\phi)} \right] \quad (22)$$

Substituting α_1 in equation 17,

$$\hat{I}_{m1} = (1 - \omega^2 \cdot C_f \cdot L_g) \cdot \sqrt{(\hat{I}_g \cdot \cos(\phi))^2 + \left[\hat{I}_g \cdot \sin(\phi) - \frac{\omega \cdot C_f}{1 - \omega^2 \cdot C_f \cdot L_g} \cdot \hat{V}_g \right]^2} \quad (23)$$

Substituting equation 22 and 23 in 7,

$$i_{m1}(t) = (1 - \omega^2 \cdot C_f \cdot L_g) \cdot \hat{I}_g \cdot \cos(\omega \cdot t + \phi) + \omega \cdot C_f \cdot \hat{V}_g \cdot \sin(\omega \cdot t) \quad (24)$$

If only fundamental components are considered, the voltage $V_s = 0$. It consists of only the triple fundamental frequency components. Similar to derivations above, the equations from 25 to 30 are obtained.

$$V_{cf1}(s) = V_g(s) - s \cdot L_g \cdot I_g(s) \quad (25)$$

$$\hat{V}_{cf1} \cdot e^{j\beta_1} = \hat{V}_g - j \cdot \omega \cdot \hat{I}_g \cdot e^{j\phi} \quad (26)$$

$$\hat{V}_{cf1} \cdot \cos(\omega \cdot t + \beta_1) = \hat{V}_g \cdot \cos(\omega \cdot t) + \omega \cdot L_g \cdot \hat{I}_g \cdot \sin(\omega \cdot t + \phi) \quad (27)$$

$$\begin{pmatrix} \hat{V}_{cf1} \cdot \cos(\beta_1) \cdot \cos(\omega \cdot t) \\ \pm \hat{V}_{cf1} \cdot \sin(\beta_1) \cdot \sin(\omega \cdot t) \end{pmatrix} = \begin{pmatrix} \hat{V}_g \cdot \cos(\omega \cdot t) + \\ \omega \cdot L_g \cdot \hat{I}_g \cdot \sin(\phi) \cdot \cos(\omega \cdot t) \\ + \omega \cdot L_g \cdot \hat{I}_g \cdot \cos(\phi) \cdot \sin(\omega \cdot t) \end{pmatrix} \quad (28)$$

$$\beta_1 = \operatorname{arccot} \left[\frac{\hat{V}_g}{\omega \cdot L_g \cdot \hat{I}_g \cdot \cos(\phi)} + \tan(\phi) \right] \quad (29)$$

$$\hat{V}_{cf1} = \omega \cdot L_g \cdot \sqrt{(\hat{I}_g \cdot \cos(\phi))^2 + \left[\hat{I}_g \cdot \sin(\phi) + \frac{\hat{V}_g}{\omega \cdot L_g} \right]^2} \quad (30)$$

$$v_{cf1}(t) = \hat{V}_g \cdot \cos(\omega \cdot t) - \omega \cdot L_g \cdot \sin(\omega \cdot t - \phi) \quad (31)$$

Considering the $3 \cdot \omega$ system, the grid current I_g does not consist of triple fundamental component. The filter capacitor voltage v_{cf} corresponds to negative of the star point voltage v_s .

$$\begin{aligned} v_s(t) &= \hat{V}_s \cdot \cos(3\omega \cdot t + \theta) \\ i_{m3}(t) &= \hat{I}_{m3} \cdot \cos(3\omega \cdot t + \alpha_3) \\ v_{cf3}(t) &= \hat{V}_{cf3} \cdot \cos(3\omega \cdot t + \beta_3) \\ v_{b3}(t) &= \hat{V}_{b3} \cdot \cos(3\omega \cdot t + \gamma_3) \end{aligned} \quad (32)$$

The phase angle θ is equal to angle β_3 and the peak voltage \hat{V}_{cf3} is equal to $-\hat{V}_s$. From the Fig. 2, the equations 33 and 34 are obtained.

$$V_{cf3}(s) = -\frac{1}{s \cdot C_f} \cdot I_{m3}(s) \quad (33)$$

$$V_{b3}(s) = -s \cdot L_m \cdot I_{m3}(s) + V_{cf3}(s) \quad (34)$$

Substituting equation 33 in 34,

$$V_{b3}(s) = (s^2 \cdot C_f \cdot L_m + 1) \cdot V_{cf3}(s) \quad (35)$$

$$\hat{V}_{b3} \cdot e^{j\gamma_3} = -(1 - 9 \cdot \omega^2 \cdot C_f \cdot L_m) \cdot \hat{V}_s \cdot e^{j\theta} \quad (36)$$

$$\hat{V}_{b3} \cdot \cos(3\omega \cdot t + \gamma_3) = -(1 - 9 \cdot \omega^2 \cdot C_f \cdot L_m) \cdot (\hat{V}_s \cdot \cos(3\omega \cdot t + \theta)) \quad (37)$$

$$\begin{pmatrix} \hat{V}_{b3} \cdot \cos(\gamma_3) \cdot \cos(3\omega \cdot t) \\ -\hat{V}_{b3} \cdot \sin(\gamma_3) \cdot \sin(3\omega \cdot t) \end{pmatrix} = -(1 - 9 \cdot \omega^2 \cdot C_f \cdot L_m) \begin{pmatrix} \hat{V}_s \cdot \cos(\theta) \cdot \cos(3\omega \cdot t) \\ -\hat{V}_s \cdot \sin(\theta) \cdot \sin(3\omega \cdot t) \end{pmatrix} \quad (38)$$

Solving equation 38, the angle γ_3 and peak voltage \hat{V}_{b3} are obtained.

$$\begin{aligned} \gamma_3 &= \theta \\ \hat{V}_{b3} &= -(1 - 9 \cdot \omega^2 \cdot C_f \cdot L_m) \cdot \hat{V}_s \end{aligned} \quad (39)$$

From equation 33,

$$I_{m3}(s) = -s \cdot C_f \cdot V_{cf3}(s) \quad (40)$$

$$\hat{I}_{m3} \cdot e^{j\alpha_3} = j \cdot 3\omega \cdot C_f \cdot \hat{V}_s \cdot e^{j\theta} \quad (41)$$

$$\hat{I}_{m3} \cdot \cos(3\omega \cdot t + \alpha_3) = -3 \cdot \omega \cdot C_f \cdot \hat{V}_s \cdot \sin(3\omega \cdot t + \theta) \quad (42)$$

$$\begin{pmatrix} \hat{I}_{m3} \cdot \cos(\alpha_3) \cdot \cos(3\omega \cdot t) \\ -\hat{I}_{m3} \cdot \sin(\alpha_3) \cdot \sin(3\omega \cdot t) \end{pmatrix} = -(3\omega \cdot C_f) \begin{pmatrix} \hat{V}_s \cdot \sin(\theta) \cdot \cos(3\omega \cdot t) \\ +\hat{V}_s \cdot \cos(\theta) \cdot \sin(3\omega \cdot t) \end{pmatrix} \quad (43)$$

Solving equation 43, the angle α_3 and peak voltage \hat{I}_{m3} and $i_{m3}(t)$ are obtained.

$$\alpha_3 = \theta - \text{sign}(\theta) \cdot \frac{\pi}{2} \quad (44)$$

$$\hat{I}_{m3} = -3\omega \cdot C_f \cdot \hat{V}_s \cdot \text{sign}(\theta) \quad (45)$$

$$i_{m3}(t) = -3\omega \cdot C_f \cdot \hat{V}_s \cdot \sin(3\omega \cdot t + \theta) \quad (46)$$

The normalized instantaneous bridge current $i_m(t)$ is obtained by adding the fundamental $i_{m1}(t)$ and triple fundamental frequency component $i_{m3}(t)$ and dividing with \hat{V}_g .

$$\frac{i_m(t)}{\hat{V}_g} = (1 - \omega^2 \cdot C_f \cdot L_g) \cdot \frac{\hat{I}_g}{\hat{V}_g} \cdot \cos(\omega \cdot t + \phi) + \omega \cdot C_f \cdot \sin(\omega \cdot t) - 3\omega \cdot C_f \cdot \frac{\hat{V}_s}{\hat{V}_g} \cdot \sin(3\omega \cdot t + \theta) \quad (47)$$

Similarly, the normalized instantaneous bridge voltage $v_b(t)$ is obtained by adding the fundamental $v_{b1}(t)$ and triple fundamental frequency component $v_{b3}(t)$ and dividing with \hat{V}_g .

$$\frac{v_b(t)}{\hat{V}_g} = \left(\begin{array}{l} \omega \cdot (L_m + L_g - \omega^2 \cdot C_f \cdot L_m \cdot L_g) \cdot \frac{\hat{I}_g}{\hat{V}_g} \cdot \sin(\omega \cdot t + \phi) + (1 - \omega^2 \cdot C_f \cdot L_m) \cdot \cos(\omega \cdot t) \dots \\ - (1 - 9\omega^2 \cdot C_f \cdot L_m) \cdot \frac{\hat{V}_s}{\hat{V}_g} \cdot \cos(3\omega \cdot t + \theta) \end{array} \right) \quad (48)$$

The resultant instantaneous bridge power obtained by multiplication of $i_m(t)$ and $v_b(t)$ is shown in equation 49. This instantaneous power should not be allowed to be negative. The integral in equation 50 must be zero.

$$p(\hat{I}_g, \hat{V}_s, \theta, \omega, t) = \left(\begin{array}{l} \left(\begin{array}{l} (1 - \omega^2 \cdot C_f \cdot L_g) \cdot \frac{\hat{I}_g}{\hat{V}_g} \cdot \cos(\omega \cdot t + \phi) \dots \\ + \omega \cdot C_f \left(\sin(\omega \cdot t) - 3 \cdot \frac{\hat{V}_s}{\hat{V}_g} \cdot \sin(3\omega \cdot t + \theta) \right) \end{array} \right) \dots \\ \cdot \left(\begin{array}{l} \omega \cdot (L_m + L_g - \omega^2 \cdot C_f \cdot L_m \cdot L_g) \cdot \frac{\hat{I}_g}{\hat{V}_g} \cdot \sin(\omega \cdot t + \phi) \dots \\ + (1 - \omega^2 \cdot C_f \cdot L_m) \cdot \cos(\omega \cdot t) \dots \\ - (1 - 9 \cdot \omega^2 \cdot C_f \cdot L_m) \cdot \frac{\hat{V}_s}{\hat{V}_g} \cdot \cos(3\omega \cdot t + \theta) \end{array} \right) \end{array} \right) \quad (49)$$

$$W_{neg}(\hat{I}_g, \hat{V}_s, \theta) = \int_{-\frac{\pi}{2}}^{\frac{\pi}{2}} \min(p(\hat{I}_g, \hat{V}_s, \theta, \omega, t), 0) dt = 0 \quad (50)$$

The equation 50 should be solved for the condition of minimum $v_b(t)$ since gives the minimum DC link voltage. But an algebraic solution is not possible. The following numerical function for θ based on the specified filter parameters in the table I was derived with the help of a MATLAB®[5] optimizer.

$$\theta\left(\frac{\hat{I}_g}{\hat{V}_g}, \phi\right) = \left[2.95451 - \frac{0.00359081}{\left(\frac{\hat{I}_g}{\hat{V}_g}\right)^{\frac{3}{2}}} \right] \cdot \sin \left[3 \cdot \phi - 0.0390231 - 0.895995 \cdot e^{-16.4368 \cdot \frac{\hat{I}_g}{\hat{V}_g}} \right. \\ \left. + \frac{0.00285748}{\left(\frac{\hat{I}_g}{\hat{V}_g} - 0.009\right)} \right] - 3.94467 \cdot e^{-53.4745 \cdot \frac{\hat{I}_g}{\hat{V}_g}} + 3.02304 \quad (51)$$

Current control of the 3L-PFC

A simplified block diagram of the current controller is shown in Fig. 7. The current controller mainly consists of two blocks namely 'reference value generation through star point modulation' (hereafter SPM) and 'state space controller'. In this publication, only the SPM block is elaborated. The grid current

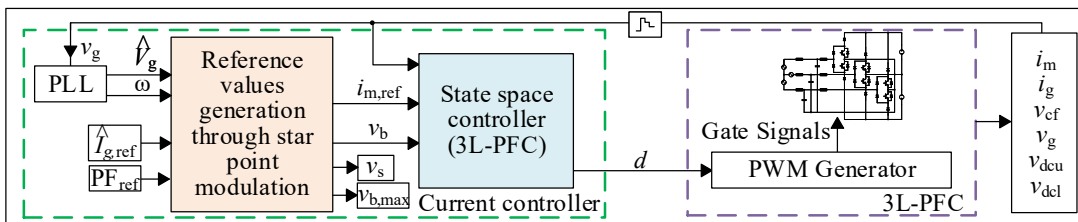


Fig. 7: Current controller of the 3L-PFC

I_g controller (marked in green dotted block) in Fig. 7 applies the duty cycle to the PWM generator of the 3L-PFC. The discretized values of the parameters i_m , i_g , v_{cf} , v_g , v_{dcu} and v_{dcl} are fed to the current controller. The SPM block requires peak value of the grid voltage, ω , reference values for grid current and power factor. The SPM generates the v_s , θ , reference bridge current $i_{m,ref}$ depending on the grid current $i_{g,ref}$ for a desired phase angle ϕ and keeping the bridge voltage v_b to a minimum value. Lower DC link voltage results in lower losses in the IGBTs and smaller ripple in the current i_m . The SPM consists of two look up tables for bridge voltage and star point voltage identification. The value of θ is calculated by fit function derived from the W_{neg} optimizer.

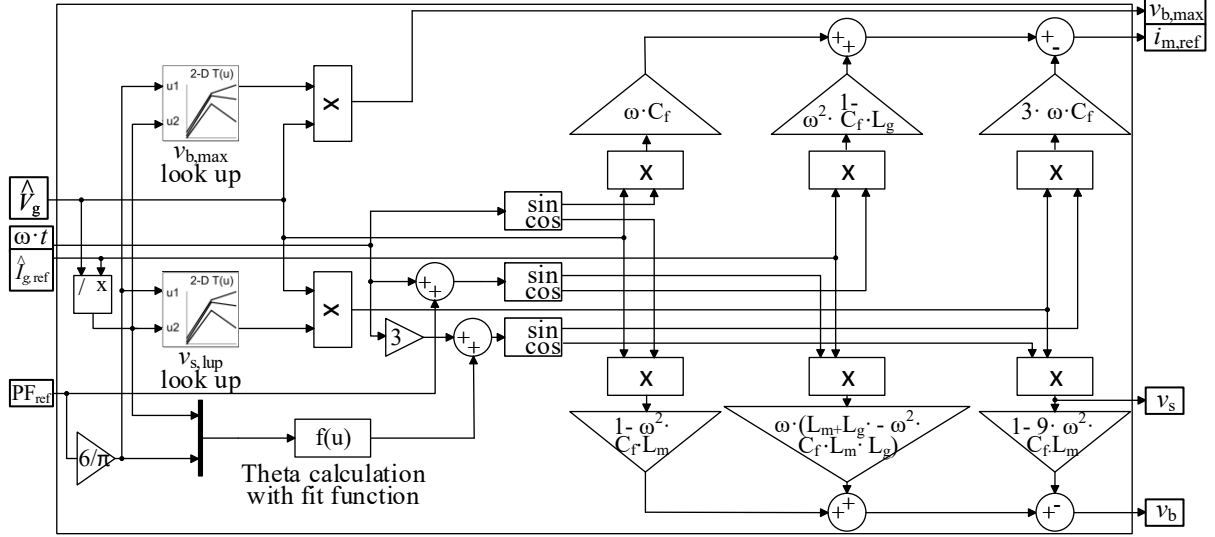


Fig. 8: Reference value generation through star point modulation

Based on the equations derived previously, the look up tables obtained are shown in Fig 9, Fig. 10 and Fig. 11 for deriving the values of v_s , $v_{b,max}$ and θ respectively. $v_{b,max}$ is lower limit for V_{dcu} or V_{dcl} . Each plot contains set of values for different ratios of \hat{I}_g/\hat{V}_g from 0.05/ohm to 0.15/ohm. After curve fitting these individual plots, the blocks V_b minimizer and W_{neg} optimizer are formulated.

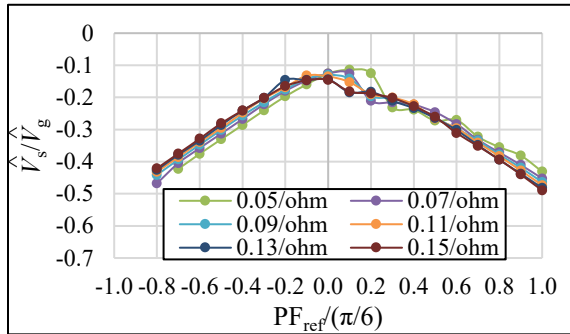


Fig. 9: $\frac{\hat{V}_s}{\hat{V}_g}$ function of $PF_{ref}/\frac{\pi}{6}$ with parameter $\frac{\hat{I}_g}{\hat{V}_g}$

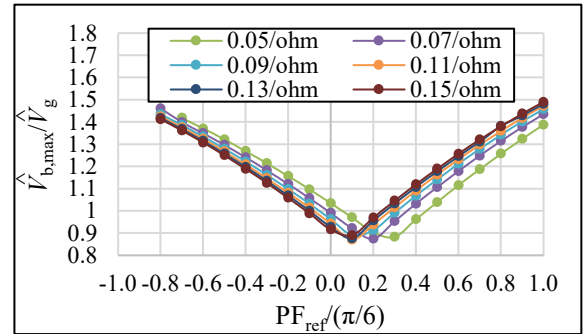


Fig. 10: $\frac{\hat{V}_{b,max}}{\hat{V}_g}$ function of $PF_{ref}/\frac{\pi}{6}$ with parameter $\frac{\hat{I}_g}{\hat{V}_g}$

The W_{neg} optimizer sets the value for the star-point voltage and the v_b minimizer sets the maximum bridge voltage to a minimum value to satisfy the requirements. Fig. 12 shows the two level optimizer for v_s , v_b and θ determination. The variable PF_{ref} is in the range of $-\pi/6$ to $\pi/6$ which covers the power factor from -0.866 up to +0.866. This covers the requirement specified in the standard [1] for reactive power availability of a grid connected rectifier.

second test results are shown in Fig. 14. Here a full load current of $\hat{I}_g = 42.25$ A is set. At t_1 , the PF_{ref} is zero. At t_2 , $\text{PF}_{\text{ref}} = -0.8 \cdot \frac{\pi}{6}$ and at t_3 , the $\text{PF}_{\text{ref}} = 1.0 \cdot \frac{\pi}{6}$. The DC link voltages applied in 14a and 14b are in similar pattern to the first test.

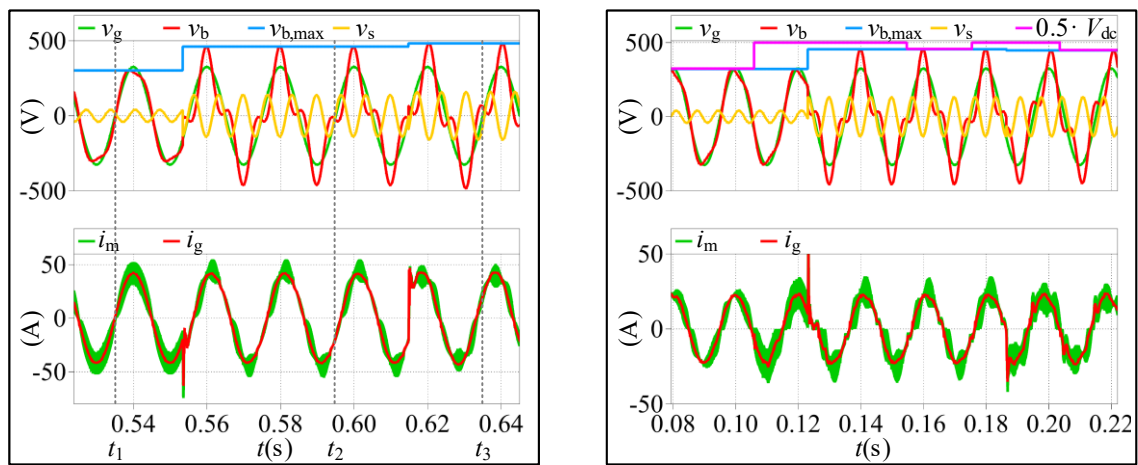


Fig. 14: $\hat{I}_g = 42.25$ A, variable PF_{ref} ; (a) with $V_{\text{dc}} = 1000$ V, (b) Minimum V_{dc} test

It is not recommended to operate the converter with a DC link voltage less than twice the minimum required bridge voltage $v_{b,\text{max}}$. This results in undesired operation of the controller causing incorrect duty cycle being applied at the PWM generator.

Conclusion and future work

The reactive power capability of the converter is proven through simulation results. In both tests, the product of the bridge voltage and bridge current always stays positive conforming to the restrictions presented by the diodes in the topology. The lagging and leading power factor between the grid voltage and grid current is also verified. The controller is to be implemented on a digital signal processor and hardware measurements are to be performed on a 20 kW PFC demonstrator developed at Fraunhofer ISE.

References

- [1] VDE-AR-N 4105.: Power Generating Plants Connected to the Low-voltage Grid, revised 2019
- [2] M. Schweizer, T. Friedli and J. W. Kolar, "Comparative Evaluation of Advanced Three-Phase Three-Level Inverter/Converter Topologies Against Two-Level Systems," in IEEE Transactions on Industrial Electronics, vol. 60, no. 12, pp. 5515-5527, Dec. 2013, doi: 10.1109/TIE.2012.2233698
- [3] J. W. Kolar and T. Friedli, "The Essence of Three-Phase PFC Rectifier Systems Part I," in IEEE Transactions on Power Electronics, vol. 28, no. 1, pp. 176-198, Jan. 2013, doi: 10.1109/TPEL.2012.2197867
- [4] M. A. Fasugba and P. T. Krein, "Gaining vehicle-to-grid benefits with unidirectional electric and plug-in hybrid vehicle chargers," 2011 IEEE Vehicle Power and Propulsion Conference, 2011, pp. 1-6, doi: 10.1109/VPPC.2011.6043207
- [5] MATLAB 2018b, The MathWorks, Inc., Natick, Massachusetts, United States.
- [6] PLECS Blockset, Plexim GmbH, Zrich, Switzerland.